CORROSION SCIENCE AND TECHNOLOGY, Vol.12, No.3(2013), pp.119~124

High-temperature Oxidation of Nano-multilayered AlTiSiN Thin Films deposited on WC-based carbides

Yeon Sang Hwang and Dong Bok Lee†

School of Advanced Materials Science and Engineering, Sungkyunkwan University, Suwon, 440-746, Korea
(Received April 09, 2013; Revised June 18, 2013; Accepted June 20, 2013)

Nano-multilayered, crystalline AlTiSiN thin films were deposited on WC-TiC-Co substrates by the cathodic arc plasma deposition. The deposited film consisted of wurtzite-type AlN, NaCl-type TiN, and tetragonal Ti_2N phases. Their oxidation characteristics were studied at 800 and 900°C for up to 20 h in air. The WC-TiC-Co oxidized fast with large weight gains. By contrast, the AlTiSiN film displayed superior oxidation resistance, due mainly to formation of the α-Al_2O_3-rich surface oxide layer, below which an (Al_2O_3, TiO_2, SiO_2)-intermixed scale existed. Their oxidation progressed primarily by the outward diffusion of nitrogen, combined with the inward transport of oxygen that gradually reacted with Al, Ti, and Si in the film.

Keywords : *AlTiSiN thin films, WC carbides, oxidation, Al_2O_3 oxide*

1. Introduction

To improve the performance and service life of cutting tools or die molds, there have been deep interests in developing new coating materials which have good mechanical, thermal and chemical properties. Presently, hard titanium nitride (TiN) films, having high hardness, corrosion-resistance and decorative color, have been successfully applied on the surfaces of mechanical components to increase the lifetime, durability and performance in abrasive and corrosive environments. However, they oxidize rapidly above 550°C owing to the formation of a TiO_2 layer.[1] Hence, the (Ti,Al)N films were developed as alternatives by partially substituting Al for Ti in TiN.[2-5] They had excellent mechanical properties such as high hardness and good wear resistance, and started to react with hot air at 700-750°C.[6] The enhanced oxidation resistance of (Ti, Al)N was attributed to the formation of an extremely thin outermost amorphous Al_2O_3 film. Below this protective film, another thin layer of TiO_2 formed on the remnant (Ti, Al)N film.[7] These results obtained from the early stage of oxidation were confirmed by Ichimura and Kawana[2] and Rebouta et al.[8]

In order to further improve the mechanical properties and oxidation resistance, (Ti,Al,Si)N films were developed.[9-15] The substitutional replacement of Al atoms in the (Ti,Al) sites resulted in a structure refinement,[13] increased hardness, mechanical properties,[16-19] and oxidation resistance.[9-11,13] (Ti,Al,Si)N films have been deposited by magnetron sputtering[9,10] and cathodic arc deposition.[11-19] Depending on the deposition methods and deposition parameters such as targets, employed gases, substrates, temperatures, and pressures, diverse (Ti,Al,Si)N film compositions (Ti- or Al-rich $Ti_{1-x}Al_xSi_yN$ with various x and y values) and structures (e.g., nanocrystalline, amorphous, TiAlN phases, *hcp*-AlN, *fcc*-AlN, *fcc*-TiN, Si_3N_4 phases) were obtained. Since the films were frequently exposed to oxidative atmospheres at high temperatures during service as wear- and corrosion-resistant ones, their oxidation characteristics are of great importance for practical applications. Therefore, the thermal stability of (Ti,Al,Si)N films was previously studied.[9-15,20] In particular, (Ti,Al,Si)N films displayed better oxidation resistance,[9-11,13] mechanical properties, and higher hardness[16-19] than (Ti,Al)N films. In order to study the thermal stability, (Ti,Al,Si)N films in the form of a homogenous single-layer or nanocomposites were heated in air,[9,11,12,15,20] low vacuum,[10,14] or nitrogen.[13] The substrates used were steel,[9,10] Si,[11,12,15] or WC-Co.[13,14] The heating were performed in the temperature range of 700-1100°C for the period of 15 min-168 h, depending on investigators. Under these oxidation conditions, the formed oxides consisted primarily of the (TiO_2,Al_2O_3,SiO_2)-mixed layer,[9] an outer Al_2O_3 layer plus an inner (TiO_2,Al_2O_3,SiO_2)-mixed

† Corresponding author: dlee@skku.ac.kr

layer,[10] an outer Al_2O_3 layer plus an inner TiO_2-rich layer,[11] an Al_2O_3 layer,[12] an outer Al_2O_3 layer plus an inner (TiO_2,Al_2O_3)-mixed layer,[13] and an outer TiO_2 layer plus an inner Al_2O_3 layer.[20] Likewise, the high-temperature oxidation of the Ti, Al and Si in the (Ti,Al,Si)N films generally resulted in the formation of complex oxides of TiO_2, Al_2O_3 and SiO_2 on the surface, respectively, which limited the diffusion of oxygen into the films.

However, more oxidation tests are needed for potential application of the (Ti,Al,Si)N film. In this study, multilayered AlTiSiN films consisting of TiN nanolayers and AlSiN nanolayers were deposited using Ti and AlSi cathodes on the WC-TiC-Co substrate by the cathodic arc plasma deposition (CAPD). Nano-multilayered films are of increasing interest for their superior mechanical and lubrication properties in advanced tribological applications. WC-based carbides, consisting of hard WC particles bound by the Co binder phase, have been used as cutting tools, rock drill tips and other wear resistant components for decades. The addition of TiC in WC–Co enhances hardness and wear resistance. In this study, the oxidation behavior of nano-multilayered AlTiSiN thin films was examined at 800 and 900°C in air. This study aims to study the oxidation kinetics, oxidation mechanism and microstructure of nano-multilayered AlTiSiN thin films. The oxidation mechanism of (Ti,Al,Si)N films under various conditions still needs to be understood further, because the oxidation behavior of the films depends sensitively on the deposition method and deposition parameters, which affect their crystallinity, composition, stoichiometry, thickness, surface roughness, grain size and orientation.

2. Experimental

AlTiSiN films were deposited on WC-20wt.%TiC -10wt.%Co sintered carbides with a size of 10x10x5 mm^3 by CAPD using pure Ti and 88 at.%Al-12 at.%Si cathodes. Detailed deposition parameters are described elsewhere.[20] Prior to deposition, a titanium interlayer was deposited with a thickness of approximately 500 nm to enhance film adhesion. The films were deposited to a thickness of about 6 μm at a nitrogen pressure of 0.4 Pa, a temperature of 250 °C, a bias voltage of -100 V, a Ti cathode arc current of 55 A, and a Al-Si cathode arc current of 35 A. The substrate holder was rotated with a speed of 4.55 rpm during deposition. Nano-multilayered films were attained by rotating the substrate between two opposed cathodes of Ti and Al-Si. The average film composition was 26.6Al-10.7 Ti-3.3Si-59.4N (at.%) according to the electron probe microanalysis (EPMA).

The AlTiSiN films were oxidized at 800 and 900°C for up to 20 h in 1 atm of air. Using a thermogravimetric analyzer, weight gains were measured continuously as a function of time during oxidation. Following oxidation, the films were inspected by EPMA, a field-emission scanning electron microscope (FE-SEM), an X-ray diffractometer (XRD) with Cu-Kα radiation, an Auger electron spectrometer (AES), and a transmission electron microscope (TEM operated at 200 keV) equipped with an energy dispersive spectrometer (EDS with 5 nm spot size).

3. Results and discussion

Fig. 1. shows FE-SEM/EPMA/TEM/XRD results of the prepared AlTiSiN film. The smooth film surface consisted of numerous small, round, nanometer-size grains (Fig. 1(a)). The film exhibited brittle fracture (Fig. 1(b)). It was thin, dense, and adherent to the substrate (Fig. 1(c)). The corresponding EPMA line profiles differentiated the AlTiSiN film, the Ti-interlayer, and the WC-TiC-Co carbides (Fig. 1(d)). The TEM cross-sectional image of the film revealed a nano-multilayered structure (Fig. 1(e)). Here, white layers were AlSiN (width = 8 nm), which originated from the 88 at.%Al-12 at.%Si cathode, and dark layers were Ti-N (width = 3 nm), originating from the Ti cathode. The unequal thickness of these alternating nano-multilayers may be related with the different deposition yield, solubility and mobility of Al, Ti, and Si. In Fig. 1(f), the substrate patterns of α-WC and the TiC additive were strong, owing to the thinness of the as-deposited film that consisted primarily of wurtzite-type AlN, NaCl-type TiN, and tetragonal Ti_2N. The intensity of these phases were weak and broad because the film was nanocrystalline and multilayered.

The isothermal oxidation kinetics of WC-TiC-Co substrate and the as-deposited AlTiSiN film are shown in Fig. 2. The uncoated substrate oxidized fast with large weight gains at 800 and 900°C due mainly to the formation of the non-protective $CoWO_4$. It is known that tungsten-containing oxides are invariably highly volatile at high temperatures, eventually resulting in complete volatilization.[22] The substrate oxidized parabolically, indicating that a diffusion process controlled the oxidation reaction. By contrast, weight gains of the AlTiSiN film were almost nil at 800 and 900°C. The AlTiSiN film dramatically improved the oxidation resistance of WC-TiC-Co substrate.

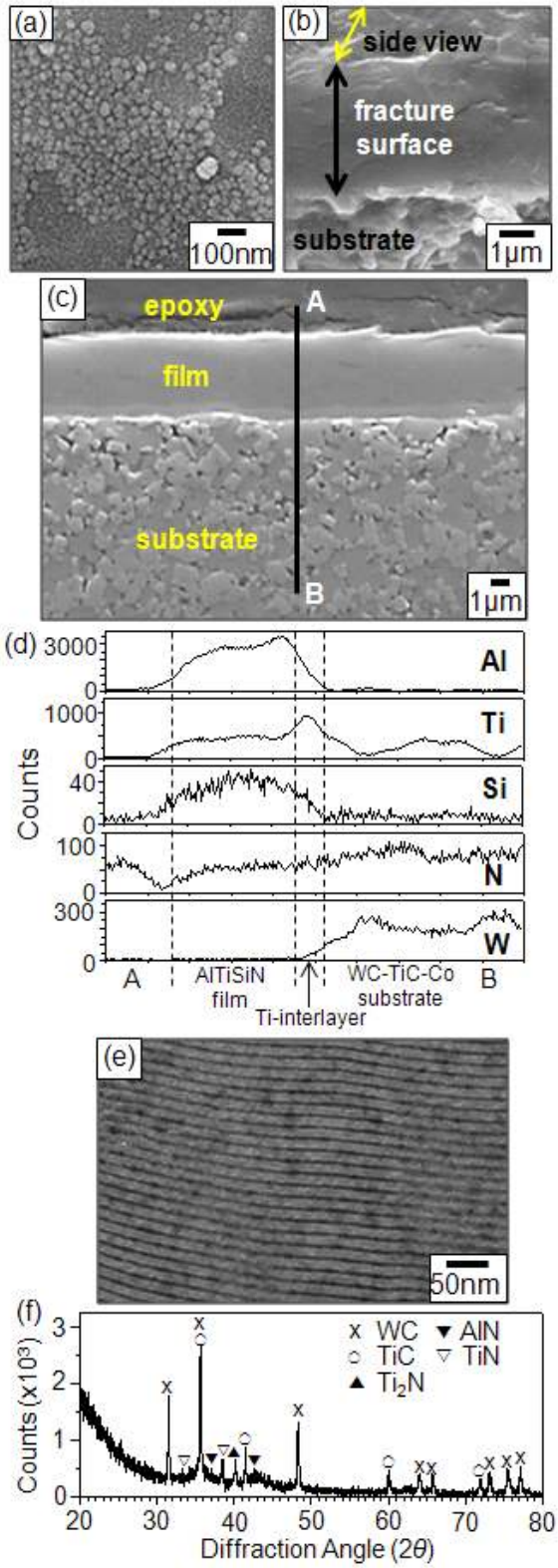

Fig. 1. AlTiSiN film deposited on the WC-TiC-Co substrate. (a) FE-SEM top view of the film, (b) FE-SEM image of the fracture surface of the film, (c) cross-sectional EPMA image, (d) line profiles of (c), (e) bright-field (BF) TEM image of the film, (f) XRD pattern.

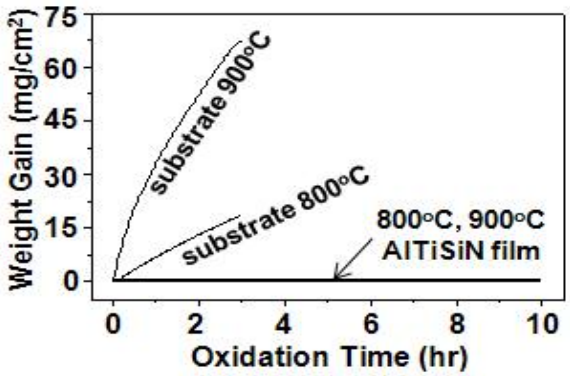

Fig. 2. Weight change vs. oxidation time curves of WC-TiC-Co substrate and AlTiSiN film at 800 and 900°C in air.

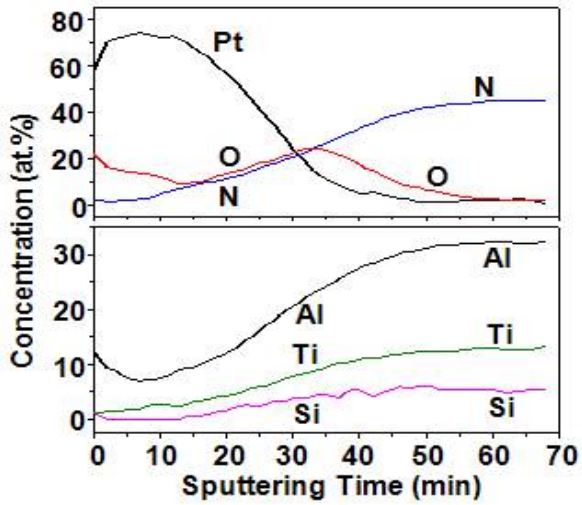

Fig. 3. AES depth profiles of the AlTiSiN film after oxidation at 800°C for 15 min in air. The penetration rate is 18 nm/min for the reference SiO_2.

Fig. 3. shows AES depth profiles of the oxidized AlTiSiN film, which was performed in order to understand the oxidation mechanism. Since a thin Pt film was sputter-deposited on top of the AlTiSiN film prior to oxidation, the maximum concentration point of the inert Pt marker corresponded to the original sample surface. It is seen that nitrogen diffused outwardly to escape from the surface probably as N_2 gas, while oxygen diffused inwardly to react with Al, Ti, and Si, as TiN/AlN nano-multilayer[5] and TiAlSiN films[10,11] did during oxidation. Although most of the scale formed by the inwardly transported oxygen, the outermost scale formed by the outward diffusion of Al, Ti and Si. This is consistent with the following facts. α-Al_2O_3 grows primarily by the inward diffusion of oxygen along the grain boundaries, although there is some outward

growth as well.[22] TiO_2 forms by either inwardly diffusing oxygen ions or outwardly transported Ti ions. The tendency of Si to diffuse outward was the weakest, because silicon ions were relatively immobile owing to the high bonding energy of Si^{4+}-O^{-2} (465 kJ mol^{-1}),[23] and also due to the low concentration gradient of Si whose amount was the smallest in the film. It is noted that the standard free energies of formation of oxides per mole of O_2 (ΔG_f^o), for example at 800°C are as follows: α-Al_2O_3 = -891 (kJ), SiO_2 = -716 (kJ) and TiO = -878 (kJ).[24] TiO is the precursor of the thermodynamically stable TiO_2. Initially, Al, Si and Ti oxi dized competitively according to their concentration due to their highly negative ΔG_f^o values. Hence, an Al_2O_3-rich scale formed on the surface. Since α-Al_2O_3 grows very slowly on account of its highly stoichiometric structure, and the *fcc*-AlN is largely covalently bonded,[25] the oxidation of Al occurred quite slowly. Hence, the AlTiSiN film displayed superior oxidation resistance.

Fig. 4. shows the XPS spectra of the oxidized AlTiSiN film. The composition of the surface oxide scale was 33Al-5.5Ti-59.1O-2.4N (at.%), implying the formation of $(Al,Ti)_2(O,N)_3$, viz. Al_2O_3 incorporated with a small amount of Ti and nitrogen. No Si was detected owing to the relative immobility of Si^{4+} ions and the small amount of Si in the as-deposited film. Since Al was the more mobile, abundant in the film, and an active element, a protective Al_2O_3–rich surface scale formed. On the other hand, the Al_{2p} peak was centered at 74.3 eV, which matched with the binding

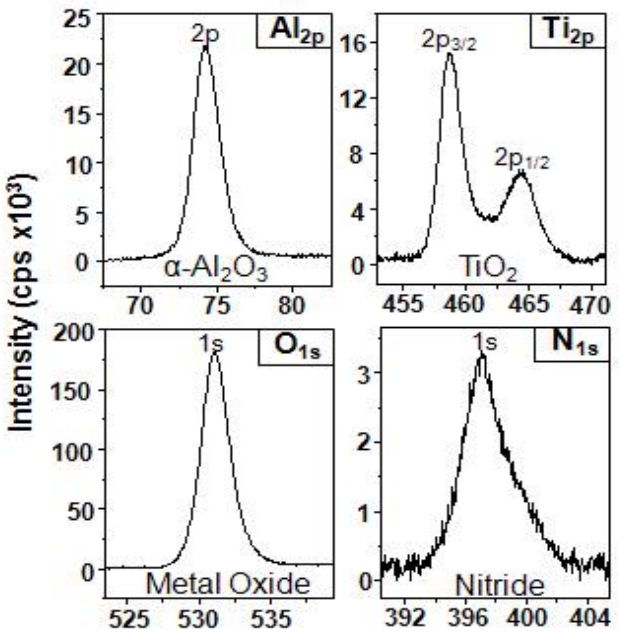

Fig. 4. XPS spectra of Al_{2p}, Ti_{2p}, O_{1s}, and N_{1s} taken from the outermost surface of the AlTiSiN film that was oxidized at 800°C for 20 h.

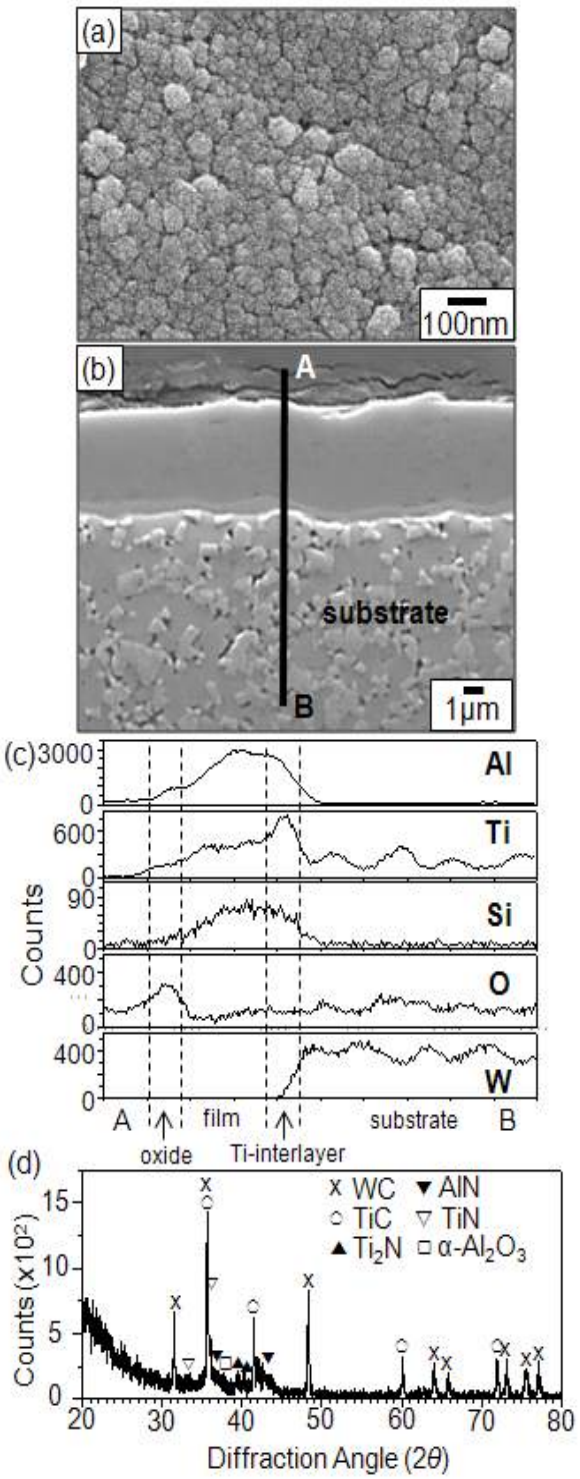

Fig. 5. AlTiSiN film after oxidation at 800°C for 20 h. (a) FE-SEM top view, (b) EPMA cross-sectional image, (c) line profiles along A-B shown on (b), (d) XRD pattern.

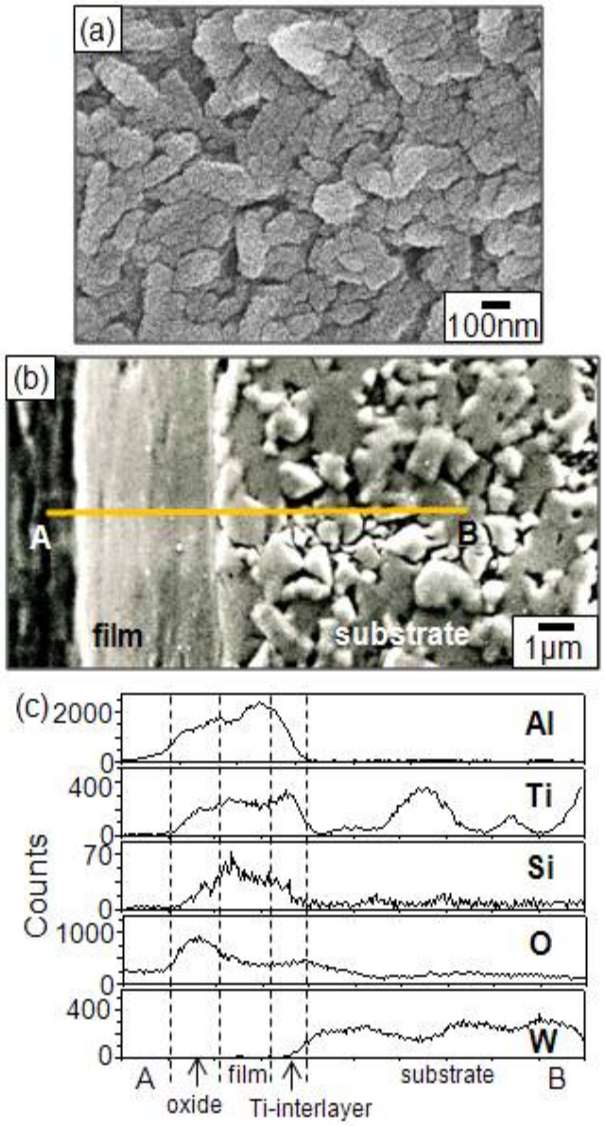

Fig. 6. AlTiSiN film after oxidation at 900°C for 10 h. (a) FE-SEM top view, (b) EPMA cross-sectional image, (c) line profiles across A and B of (b).

energy of Al_2O_3. The $Ti_{2p3/2}$ spectrum showed a component at 458.8 eV, implying the formation of TiO_2. The O_{1s} spectrum shows a binding energy component at 531.3 eV associated with oxygen in metal oxides. In contrast with the strong O_{1s} spectrum, the N_{1s} spectrum (E_b =398.4 eV) was weak owing to the liberation of nitrogen. The release of nitrogen from the film may deter the formation of dense, continuous protective scales.

Fig. 5. shows the SEM/EPMA/XRD results of the AlTiSiN film after oxidation at 800°C for 20 h. The surface scale consisted of numerous, tiny oxide crystallites originating from the formation of slowly growing oxides (Fig. 5(a)). The EPMA results shown in Figs. 5(b) and (c) revealed the oxide scale that formed on the AlTiSiN film, below which the Ti-interlayer and the WC-TiC-Co substrate existed. The highly protective Al_2O_3-rich scale was dense and about 2 μm-thick. The nitrogen line profile shown in Fig. 5(c) indicated the release of nitrogen around the oxide scale. Fig. 5(d) shows the (α–WC, TiC)-substrate and the as-deposited film that consisted primarily of wurtzite-type AlN, NaCl-type TiN, and tetragonal Ti_2N. The strong substrate peaks and the weak α-Al_2O_3 peak indicated that oxidation progressed to a small extent.
Fig. 6. shows the SEM/EPMA results of the AlTiSiN film after oxidation at 900°C for 10 h. The surface oxide grains grew to a round shape, but they were still sub-micrometer in size (Fig. 6(a)). The EPMA results shown in Figs. 6(b) and (c) revealed about 3 μm-thick Al_2O_3-rich oxide scale, the AlTiSiN film, the Ti-interlayer, and the WC-TiC-Co substrate. The film had a good oxidation resistance at 900°C.

4. Conclusions

The oxidation behavior of AlTiSiN nano-multilayered thin films deposited on a WC-TiC-Co substrate was investigated at 800 and 900°C in air. The film which was composed of wurtzite-type AlN, NaCl-type TiN, and tetragonal Ti_2N phases displayed excellent oxidation resistance. Since Al had a high affinity for oxygen and its amount was the largest in the film, an α-Al_2O_3–rich surface scale formed, which was responsible for the excellent oxidation resistance. Below the α-Al_2O_3–rich surface scale, a thin (Al_2O_3, TiO_2, SiO_2)-intermixed scale formed by the inwardly diffusing oxygen. Si was relatively immobile. During oxidation, oxygen from the atmosphere diffused inwardly, whereas nitrogen diffused outwardly.

Acknowledgments

This research was supported by Basic Science Research Program through the National Research Foundation of Korea (NRF) funded by the Korean Ministry of Education, Science and Technology (2010-0023002).

References

1. I. Milošev, H. H. Strehblow and B. Navinšek, *Thin Solid Films*, **303**, 246 (1997).
2. H. Ichimura and A. Kawana, *J. Mater. Res.*, **8**, 1093 (1993).
3. S. H. Yao, Y. L. Su, W. H. Kao and T. H. Liu, *Tribol.*

Int., **39**, 332 (2006).
4. D. G. Kim, T. Y. Seong and Y. J. Baik, *Thin Solid Films*, **397**, 203 (2001).
5. Y. H. Jeong, D. M. Kwang, C. H. Chung, W. G. Kim and H. C. Choe, *Corros. Sci. Tech.*, **10**, 212 (2011).
6. W. D. Münz, *J. Vac. Sci. Technol*., **A4,** 2695 (1986).
7. D. McIntyre, J. E. Greene, G. Hakansson, J. E. Sundgren and W. D. Münz, *J. Appl. Phys.*, **67**, 1542 (1990).
8. L. Rebouta, F. Vaz, M. Andritschky and M. F. Da Silva, *Surf. Coat. Technol.*, **70**, 76 (1995).
9. F. Vaz, L. Rebouta, M. Andritschky, M. F. Da Silva and J. C. Soares, *Surf. Coat. Technol.*, **98**, 912 (1998).
10. A. Vennemann, H. R. Stock, J. Kohlscheen, S. Rambadt and G. Erkens, *Surf. Coat. Technol.*, **408**, 174 (2003).
11. M. Pfeiler, J. Zechner, M. Penoy, C. Michotte, C. Mitterer and M. Kathrein, *Surf. Coat. Technol.*, **203**, 3104 (2009).
12. Y. Y. Chang and S. M. Yang, *Thin Solid Films*, **518**, s34 (2010).
13. M. Parlinska-Wojtan, A. Karimi, O. Coddet, T. Cselle and M. Morstein, *Surf. Coat. Technol.*, **344**, 188 (2004).
14. A. Flink, J.M. Andersson, B. Alling, R. Daniel, J. Sjölén, L. Karlsson and L. Hultman, *Thin Solid Films*, **517**, 714 (2008).
15. N. Fukumoto, H. Ezura and T. Suzuki, *Surf. Coat. Technol.*, **204**, 902 (2009).
16. Y. Tanaka, N. Ichimiya, Y. Onishi and Y. Yamada, *Surf. Coat. Technol.*, **215**, 146 (2001).
17. O. Durand-Drouhin, A. E. Santana, A. Karimi, V. H. Derflinger and A. Schütze, *Surf. Coat. Technol.*, **260**, 163 (2003).
18. P. J. Martin, A. Bendavid, J. M. Cairney and M. Hoffman, *Surf. Coat. Technol.*, **200**, 2228 (2005).
19. S. Q. Wang, L. Chen, B. Yang, K. K. Chang, Y. Du, J. Li and T. Gang, *Int. J. Refract. Met. Hard Mater.*, **28**, 593 (2010).
20. Y. Y. Chang, *J. Nanosci. Nanotechno.*, **10**, 4762 (2010).
21. S. K. Kim, P. V. Vinh, J. H. Kim and T. Ngoc, *Surf. Coat. Technol.*, **200**, 1391 (2005).
22. N. Birks, G. H. Meier and F. S. Pettit, *Introduction to the High-Temperature of Metals*, 2nd ed, Cambridge University Press, England (2006).
23. P. Kofstad, *Oxid. Met.*, **44**, 3 (1995).
24. I. Barin, *Thermochemical Data of Pure Substances*, VCH, Weinhein, Germany (1989).
25. H. Holleck, *J. Vac. Sci. Technol.*, **A4**, 2661 (1986).